AGU ADVANCING EARTH AND SPACE SCIENCES

Geophysical Research Letters®

Key Points:

- The free energy and thermoelasticity of FeH_x were investigated using ab initio molecular dynamics under the Earth's inner core conditions
- FeH_x adopts an hexagonal close-packed structure at the high temperatures of the Earth's inner core
- Superionic H can explain the inner core seismic characteristics

Supporting Information:

Supporting Information may be found in the online version of this article.

Correspondence to:

Y. Li and F. Zhang,
liyunguo@ustc.edu.cn;
zhangfeiwu@vip.gyig.ac.cn

Author Contributions:

Conceptualization: Yunguo Li, Feiwu Zhang
Data curation: Hua Yang, Tingting Xiao
Formal analysis: Hua Yang, Tingting Xiao, Yunguo Li, Joshua M. R. Muir, Feiwu Zhang
Funding acquisition: Yunguo Li, Joshua M. R. Muir, Feiwu Zhang
Investigation: Hua Yang, Peixue Dou, Tingting Xiao
Methodology: Hua Yang, Peixue Dou, Tingting Xiao, Joshua M. R. Muir
Project Administration: Yunguo Li, Feiwu Zhang
Software: Hua Yang, Tingting Xiao
Supervision: Yunguo Li, Feiwu Zhang
Validation: Yunguo Li, Feiwu Zhang

The Geophysical Properties of FeHx Phases Under Inner Core Conditions

Hua Yang[1], Peixue Dou[2,3], Tingting Xiao[2,3], Yunguo Li[2,3] , Joshua M. R. Muir[1] , and Feiwu Zhang[1]

[1]State Key Laboratory of Ore Deposit Geochemistry, Institute of Geochemistry, Chinese Academy of Sciences, Guiyang, China, [2]School of Earth and Space Sciences/Deep Space Exploration Laboratory, University of Science and Technology of China, Hefei, China, [3]CAS Key Laboratory of Crust-Mantle Materials and Environments/CAS Center for Excellence in Comparative Planetology, University of Science and Technology of China, Hefei, China

Abstract Hydrogen has been proposed as an important light element in planetary iron cores, while the crystal structure and thermoelasticity of FeH_x ($x = 1$) (FeH hereafter) under inner core conditions remain largely unknown. Recent studies report that FeH adopts an face-centered cubic (fcc) structure up to core conditions. In this study, using ab initio molecular dynamics, we calculate the free energy and elastic properties of FeH at high P-T conditions. Our results indicate that the hexagonal close-packed (hcp) structure of FeH_x is favored by both the low hydrogen concentration and the elevated temperature of inner-core conditions. We also clarify that lattice hydrogen hardens the wave velocities of iron while superionic hydrogen softens it. Both fcc- and hcp-FeH can match inner-core wave velocities and Poisson's ratio, which supports the hypothesis of hydrogen as a vital light element in the Earth's core.

Plain Language Summary The properties of H-bearing iron alloys under inner core conditions have been sparsely studied. Here, we calculated the energy difference between face-centered cubic (fcc) and hexagonal close-packed (hcp) FeH_x as a function of hydrogen concentration at static conditions ($T = 0$ K). We found that FeH_x exhibits hcp structure in H-poor conditions ($x < 0.8$) and fcc in H-rich conditions ($x > 0.8$) at high pressures. Further Gibbs free energy calculations suggest that the hcp phase is favored at the temperature of Earth's inner core. The inner core hydrogen content was constrained to be ~0.26–0.34 wt% based on fcc H-bearing Fe alloy's equations of state. Finally, we calculated the elasticity of FeH (an iron lattice surrounded by superionic hydrogen) and found that the addition of superionic hydrogen dramatically decreased the shear modulus G and shear wave velocities V_s of iron at high temperatures of the inner core. The real core has sound velocities lower than those of pure iron and thus FeH_x with superionic hydrogen is a promising core candidate.

1. Introduction

The Earth's core is mainly composed of an Fe-rich alloy with a small amount (~5%–10%) of light elements (e.g., Si, O, S, C, and H) being required to explain its seismic and geophysical observations (Hirose et al., 2021; Poirier, 1994). Hydrogen has been considered one of the most important light elements in the Earth's core since it has the highest abundance in the solar system (Lodders, 2003), high solubility in iron metal under high pressures (Fukai, 1984; Ohtani et al., 2005; Okuchi, 1997) as well as possessing a siderophile nature at core conditions (Iizuka-Oku et al., 2017; Li et al., 2020; Shibazaki et al., 2009; Tagawa et al., 2021). Determining the structures and properties of FeH_x iron hydride is essential for understanding the chemical and physical properties of the core. However, studies aimed at determining the Fe-H phase diagram and crystal structures for geophysical applications are scarce and still controversial (Hirose et al., 2021).

Isaev et al. (2007) conducted static free energy calculations and proposed that FeH undergoes a phase transition from a double hexagonal close-packed (dhcp) to a hexagonal close-packed (hcp) structure at 37 GPa, and then a second transition from an hcp to face-centered cubic (fcc) structure was observed at 83 GPa. Further compressional experiments suggested that dhcp FeH can be stable up to 136 GPa at ambient temperature (Pépin et al., 2014). A phase transition from dhcp to fcc in FeH induced by temperature has been observed up to 20 GPa in a multi-anvil apparatus (Ikuta et al., 2019; Sakamaki et al., 2009). The hcp structure of FeH has also been found to be stable under higher P-T conditions (Oka et al., 2022; Yuan et al., 2018). Alternatively, some experiments found that FeH_x ($x \sim 1$) adopts a stable fcc structure at a wide range of high P-T conditions (~3.8–142 GPa, 750–3660 K) (Hikosaka et al., 2022; Ikuta et al., 2019; Kato et al., 2020; Narygina et al., 2011; Pépin et al., 2014;

Writing – original draft: Hua Yang, Peixue Dou, Tingting Xiao
Writing – review & editing: Peixue Dou, Yunguo Li, Joshua M. R. Muir, Feiwu Zhang

Tagawa et al., 2022a; Thompson et al., 2018), which suggest that fcc FeH is a likely candidate component of the Earth's core. However, all of these predictions are based on extrapolations of observations at temperatures and pressures much lower than those of the inner core and therefore, the real structure of FeH in the Earth's inner core is still under debate and needs to be investigated. At high temperatures various FeH$_x$ structures have shown superionic H behavior (He et al., 2022a; Wang et al., 2021; Yang et al., 2022a), which means low-temperature calculations and experiments are unlikely to capture the correct phase of Fe-H complexes at high temperatures. More recently, Yang et al. (2022a) proposed that fcc structure FeH could be stable at inner core conditions based on iron hydride (Fe$_x$H$_y$) structural prediction and thermodynamic property calculations. The relative stability between fcc and hcp structure FeH at inner core *P-T* conditions is still vaguely known, however.

Additionally, the seismic properties of FeH at high *P-T* conditions have only been sparsely reported. Isaev et al. (2007) calculated Debye sound velocities of fcc FeH up to ∼80 GPa. Thompson et al. (2018) measured the seismic properties of fcc FeH$_x$ (x ∼1) in Nuclear Resonant Inelastic X-Ray Scattering experiments up to ∼82 GPa. Wakamatsu et al. (2022) determined the compressional wave velocities of fcc FeH with picosecond acoustic measurements in laser-heated diamond anvil cells (LHDAC) at pressures up to 100 GPa. All of these studies, however, were conducted at ambient temperatures but the effect of temperature is likely to be critical in Fe-H systems. This can be demonstrated through consideration of the seismicity of hcp Fe-H alloys. Caracas (2015a) performed static first-principle (i.e., *T* = 0 K) calculations on the seismic properties of the hcp Fe-H system, and proposed that H is not a vital light element in the Earth's core from a geophysical sense as both the elastic modulus and sound wave velocities of hcp Fe increased by incorporation of H, which is against the geophysical requirements for light elements in the inner core. When considering the seismic properties of the same system at high temperatures with superionic H (He et al., 2022a; Wang et al., 2021) opposite conclusions were reached—the effect of H is now to soften the shear modulus of hcp Fe which is geophysically plausible. Therefore, it is urgent to study the elastic properties of FeH under inner core conditions to better understand the behavior of H in the Earth's inner core.

In this study, to investigate the crystal structure and seismic properties of FeH in the Earth's inner core, we have performed ab initio molecular dynamics (AIMD) simulations to calculate the free energy and elastic properties of FeH at inner core *P-T* conditions. We report that hcp phase FeH$_x$ is favored by low H concentrations or elevated temperatures and that superionic H in FeH could explain inner core seismology which supports that H is a vital light element in the Earth's core.

2. Computational Details

Density functional theory (Hohenberg & Kohn, 1964; Kohn & Sham, 1965) calculations were performed within the generalized gradient approximation (Perdew et al., 1996) and the projector-augmented wave method (Blöchl, 1994). The calculations were implemented in the Vienna Ab initio Simulation Package code (Kresse & Furthmüller, 1996). Fe-3p^{6}3d^{7}4s^1 and H-1s^1 were treated as valence states. Single-particle orbitals were populated according to Fermi-Dirac statistics (Mermin, 1965). A plane wave cutoff energy of 500 eV and the Monkhorst-Pack scheme (Monkhorst, 1976) with a *k*-point grid of $2\pi \times 0.05$ Å^{-1} was found to give excellent stress tensors and structural energy convergence for the Fe-H system.

A supercell ($2 \times 2 \times 2$ for fcc FeH and $2 \times 2 \times 4$ for hcp FeH) of 64 atoms was modeled. The lattice and ion positions of FeH$_x$ structures were fully relaxed at 100, 150, 200, 300, 330, and 360 GPa using the energy and force convergence criteria 1×10^{-7} eV and 1×10^{-4} eV/Å, respectively. H atoms are always positioned on the (0 0 0) octahedral site to preserve the fcc and hcp symmetry of the overall structure. At pressures below 200 GPa, all relaxations allow Fe spin polarization since the magnetism disappears at pressures above ∼40 GPa for fcc Fe-H (Tagawa et al., 2022a; Yang et al., 2023) and ∼190 GPa for hcp Fe-H (Figure S1 in Supporting Information S1). For the different octahedral sites of H atoms in FeH$_x$, we also examined the energies of different configurations and found that the energy difference between them was less than 3 meV/atom, which is negligible.

AIMD calculations were performed to verify the FeH crystal structure and calculate its properties. Electronic structure calculations were performed with a plane-wave set corresponding to a 500 eV energy cutoff and iteration convergence criterion of 1×10^{-5} eV. A $2 \times 2 \times 2$ Monkhorst-Pack (Monkhorst, 1976) *k*-point mesh sampling was adopted, which is sufficient to converge the pressure to within 0.3 GPa and the total energy within 3 meV/atom. To obtain the initial lattice parameters of FeH at the target temperatures and pressure (360 GPa),

we ran *NPT* simulations in the isothermal-isobaric ensemble for 10 picoseconds (ps) to relax the supercell using a Langevin thermostat (Schneider & Stoll, 1978). We then performed *NVT* simulations with the Nosé thermostat (Nosé, 1984) for 10 ps using the lattice parameters from *NPT* simulations at the target temperatures to ensure the pressure was maintained at 360 GPa and the structure remained under hydrostatic conditions within 0.5 GPa by manually fine-tuning the supercell parameters. A time step of 1 femtosecond (fs) was used and the time-averaged electronic free energy was converged with an accuracy of ∼1 meV/atom. Uncertainties in temperature and pressure computed using the blocking method (Flyvbjerg & Petersen, 1989) are less than 7 K and 0.1 GPa, respectively. We retrieved the mean-square displacements to ensure that we were computing solid phases with results shown in Figure S2 in Supporting Information S1.

The entropy and free energy of FeH phases were derived from molecular dynamics simulations based on the two-phase thermodynamic (2PT) method (Desjarlais, 2013; Lai et al., 2012; Lin et al., 2003) which divides the vibrational spectrum into a solid-like and gas-like part. For exact methodology details we refer to Wilson and Stixrude (2021) as we implemented their formulation of this method. To verify the results obtained from the 2PT method, we further calculated the free energies of FeH phases at 2000 K using thermodynamics integration described in Text S1 in Supporting Information S1. Then, the Gibbs free energies at other temperatures were then obtained by employing the Gibbs–Helmholtz equation $\left[\left(\frac{\partial}{\partial T}\left(\frac{G}{T}\right)\right)_P = -\frac{H}{T^2}\right]$, and the used enthalpies at different temperatures are listed in Table S1 in Supporting Information S1.

The strain-stress method was used to calculate the isothermal elastic constants. We applied four different strains (±0.01 and ±0.02) to the equilibrium supercells from the *NPT-NVT* simulations and performed the *NVT* simulations with the Nosé thermostat to obtain the stresses. The *NVT* simulations on the strained boxes were run for 10 ps and the stresses were averaged from the last 8 ps of the simulations. The results of strain-stress value were then fitted to second-order polynomials and calculated the slopes at zero strain to obtain the isothermal elastic constants (Karki et al., 2001). The adiabatic elastic constants were derived from the isothermal elastic constants. The Voigt average (Simmons & Wang, 1971) was used to calculate the adiabatic bulk modulus (K_s) and shear modulus (G), and these were then propagated to the seismic wave velocities. The thermoelasticity calculations were implemented in the toolkit developed by Li, Vočadlo, and Brodholt (2022). The errors on the elastic constants were derived from the statistical errors of stresses and listed in Table S2 in Supporting Information S1, which is less than 2% for temperatures from 2000 to 5000 K. The convergence tests confirmed that a larger supercell and longer simulation time do not change our results for the elastic properties and the free energies (Tables S3 and S4, Figures S3 and S4 in Supporting Information S1). More methodological details are given in Text S1 in Supporting Information S1.

3. Results and Discussion

3.1. FeH$_x$ Structure at High *P-T* Conditions

Data on the crystal structure and thermodynamic stability of FeH at core *P-T* conditions are scarce but currently, the most discussed structures are the fcc and hcp phases (Gomi et al., 2018; Hikosaka et al., 2022; Hirose et al., 2019; Ikuta et al., 2019; Kato et al., 2020; Tagawa et al., 2022a, 2022b; Thompson et al., 2018; Yang et al., 2022a, 2023). We first calculated the enthalpy differences between fcc and hcp phase FeH$_x$ ($x \leq 1$) as a function of H concentration to determine how the H concentration influences the phase stability at static (i.e., $T = 0$ K) conditions.

As shown in Figure 1a, with low H concentrations the hcp structure is favored but, increasing the H concentration leads to a favoring of the fcc structure, and above an H concentration of ∼1.43 wt% (FeH$_x$ with $x > 0.8$) an fcc structure is favored throughout the whole pressure range of the Earth's core. This is supported by the Fe-H binary phase diagram determined by Tagawa et al. (2022b) in their X-ray diffraction (XRD) measurements, where FeH$_x$ with $x > 0.75$ adopts an fcc structure and likely changes little with increasing pressure. Our result is also supported by a LHDAC experiment on the liquidus and subsolidus phase relations in the Fe-O-H and Fe-H systems conducted by Oka et al. (2022), which proposed that FeH$_{0.2}$ forms with the hcp structure while the stoichiometric FeH forms with the fcc structure. The enthalpy difference between fcc and hcp FeH$_x$ phases increases as the pressure increases, which leads to a greater stability gap of the phases.

It is important to note that we only considered the fcc and hcp phases of FeH$_x$ in the current study. We did not consider the dhcp phase as this has been proven to transition to fcc at high temperatures (Ikuta et al., 2019;
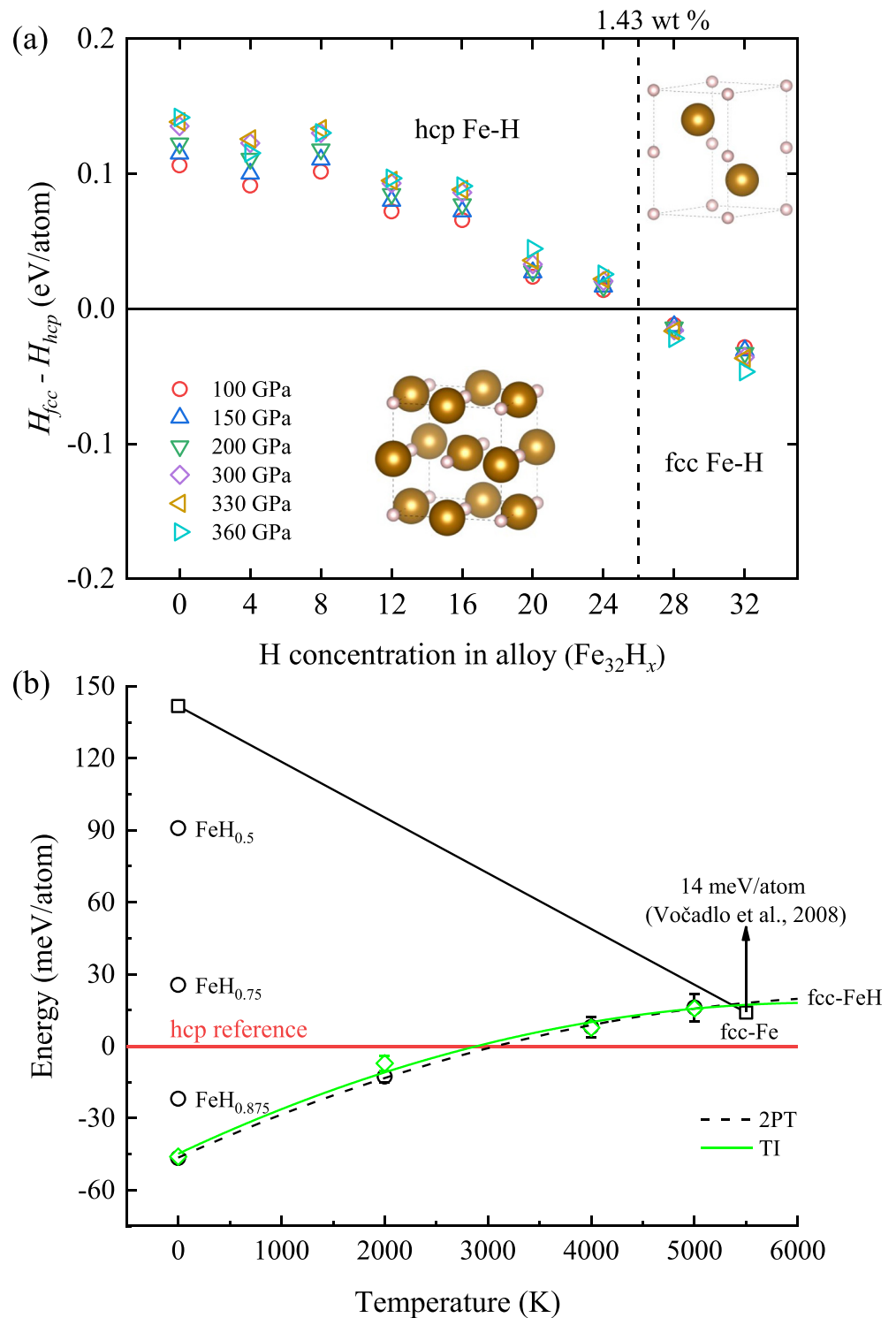
Figure 1. The energy difference between hexagonal close-packed (hcp) and face-centered cubic (fcc) FeH$_x$ ($x \leq 1$) at high *P-T* conditions. (a) Enthalpy difference as a function of H concentration at 0 K and 100–360 GPa. (b) Free energy difference between hcp- and fcc-FeH as a function of temperature at 360 GPa. Free energy difference between pure hcp- and fcc-Fe (Vočadlo et al., 2008) is also presented. The black dashed line is the fitting results of two-phase thermodynamic (2PT), while the solid green line represents the fitting results of thermodynamics integration (TI). Within uncertainties, the energy difference results obtained by these two methods are consistent. Error bars are from the statistical error of the molecular dynamics.

Kato et al., 2020; Sakamaki et al., 2009) and high pressures (Isaev et al., 2007). There is also the possibility of a body-centered cubic (bcc) FeH phase. Bcc Fe has been proposed to be stable at temperatures over 7000 K (Belonoshko et al., 2017, 2022) but we found, with the incorporation of H, bcc Fe is dynamically unstable and collapses into a tetragonal structure of FeH at our simulated Earth's inner core *P-T* conditions. This dynamic instability with the addition of H might be the reason that a bcc phase FeH has not been reported experimentally under high *P-T* conditions. Therefore, bcc FeH was also not included in the current study.

High temperatures are an important part of the inner core and can significantly affect the phase stability in the Fe-H system (Ikuta et al., 2019; Sakamaki et al., 2009). In Figure 1b, we calculated the effect of temperature on the relative stability of fcc and hcp FeH phases. The results show that as temperature increases the hcp FeH phase is increasingly favored. This is important because it means that experiments done at lower temperatures may not capture the phase structure present in the core. For example, we predict that at 2000 K fcc FeH is stable (Figure 1b) as seen by XRD experiments conducted by Kato et al. (2020) but that it becomes unstable at more core-like temperatures. However, the energy difference between these two phases at core temperatures is predicted to be very small (on the order of 10 s meV/atom), which is not massively different and could be trivial compared to the free energy differences induced by changing temperatures and compositions in the real Earth's core (Côté et al., 2008; Vočadlo et al., 2003, 2008), and thus there is a possibility of the coexistence of H-bearing hcp and fcc phases in the inner core. This supports the experimental results of Oka et al. (2022).

At temperatures above 4000 K, the diffusion coefficient of H in FeH is predicted to be as high as 10^{-8} m^2/s (Table S5 in Supporting Information S1), indicating that FeH has transformed into a liquid-like superionic state. The superionic transition temperature for H in the Fe fcc lattice is ∼500 K higher than the same transition in the hcp lattice (He et al., 2022a; Yang et al., 2022a), which means that the superionic state of the hcp phase occurs earlier than that of fcc. This may account for the faster diffusion of superionic H in the hcp lattice than in the fcc lattice at relevant *P-T* conditions. The incorporation of superionic H into hcp Fe would induce a larger total entropy than that in fcc Fe due to the earlier (lower temperature) creation of a liquid-like state (Ye et al., 2021). Therefore, although H can stabilize fcc Fe up to 3000 K, hcp FeH is more energetically favorable at high temperatures when a superionic transformation has been undergone. We can also conclude that at the Earth's inner core conditions where H concentrations are low and temperatures are high hcp FeH$_x$ ($x < 1$) phases can generally be preferred, as we observed in static conditions.

3.2. Equation of State of fcc FeH$_x$

In the following sections, we present the equation of state (EOS) and elastic properties of fcc-FeH in comparison with those of pure Fe and hcp-FeH. Coexistence of fcc-FeH$_x$ and hcp-FeH$_x$ is possible based on our thermodynamic calculations and thus establishing their seismic properties and their differences is essential to distinguish if these are different phases in the core.

We used the Birch-Murnaghan third-order EOS to fit the static *P-V* data for fcc H-bearing Fe alloys as follows:

$$P(V) = \frac{3K_0}{2}\left[\left(\frac{V_0}{V}\right)^{\frac{7}{3}} - \left(\frac{V_0}{V}\right)^{\frac{5}{3}}\right]\left\{1 + \frac{3}{4}\left(K' - 4\right)\left[\left(\frac{V_0}{V}\right)^{\frac{2}{3}} - 1\right]\right\} \tag{1}$$

where P is the pressure, V is the volume, V_0 is the initial volume, K_0 and K' are the bulk modulus at ambient pressure and its pressure derivative. The effect of H on the density of Fe thus can be evaluated. The results are shown in Table S6 in Supporting Information S1 and Figure 2, where the values from the literature are also plotted as references.

As shown in Figure 2, the initial volume V_0 increases as the H concentration increases while the bulk modulus K_0 and its pressure derivative K' decrease with increasing H concentration though the compressional behavior of H-bearing Fe is similar to that of pure Fe. This is consistent with the previous study (Caracas, 2015a) based on an hcp H-bearing Fe alloy.

The calculated equations of state were then used to match the core density deficit with H. We first used the same thermal expansion of 1.0×10^{-5} K^{-1} (Vočadlo, 2007; Vočadlo et al., 2003) for both pure Fe and H-bearing Fe alloys. The temperature of the inner core boundary (ICB) and the center is assumed to be ∼5500 and 6500 K, respectively (Anderson, 2003), which was linearly interpolated as the geotherm of the Earth's inner core. To
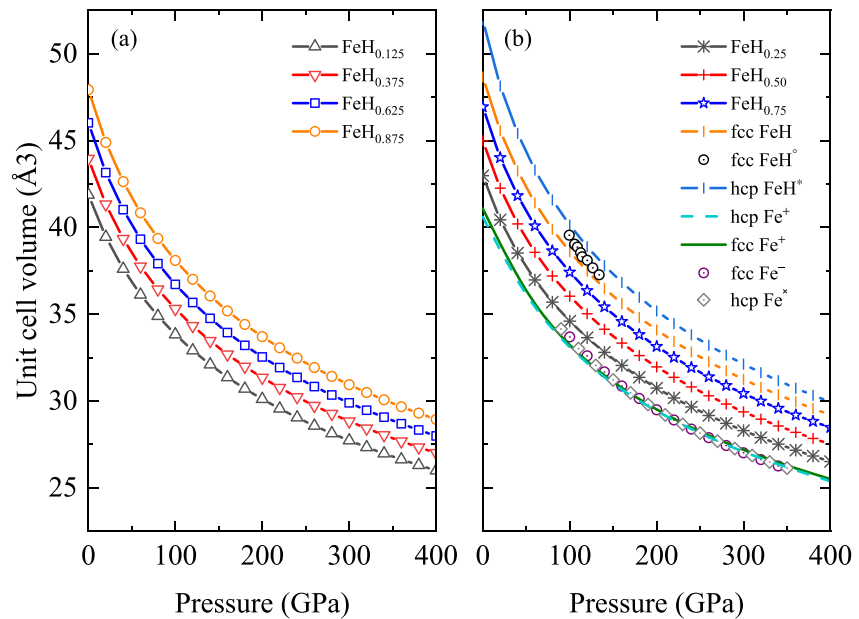
Figure 2. Compression curves of face-centered cubic (fcc) FeH$_x$ ($x \leq 1$) at static conditions: (a) for FeH$_{0.125}$, FeH$_{0.375}$, FeH$_{0.625}$, and FeH$_{0.875}$; (b) for FeH$_{0.25}$, FeH$_{0.50}$, FeH$_{0.75}$, FeH, and other data from the literature. Theoretical data with an asterisk (*) for hexagonal close-packed (hcp) FeH at 0 K from Caracas (2015a), plus (+) for hcp and fcc Fe at 0 K from Yang et al. (2022a). Experimental data points with a circle (°) for fcc FeH at 300 K from Tagawa et al. (2022a); minus (−) for fcc Fe and multiply (×) for hcp Fe at 300 K calculated from Tsujino et al. (2013) and Dewaele et al. (2006), respectively. Note that the two-unit cell volumes of hcp Fe and FeH are plotted here for comparison.

match the density of the inner core with an fcc FeH$_x$ alloy, a maximum H content of ~0.3–0.4 wt % is required as shown in Figure 3a. In order to more accurately estimate this H content, we further used the thermal expansion (1.3×10^{-5} K^{-1}) of solid FeH (1.77 wt% H) directly calculated from our MD calculations to re-constrain the inner core H content (Figure 3b) with the assumption that the thermal expansion of H-bearing Fe alloys is linear with H concentration. We ultimately estimate that the H content of the inner core to be ~0.26–0.34 wt%. This result is consistent with the recent estimate of ~0.2–0.3 wt% based on fcc H-bearing Fe alloy's equations of state by Thompson et al. (2018) and such an H content is also consistent with the ICB density jump (Li, Guo, et al., 2022).

3.3. Elasticity of H-Bearing Fe Alloys at Inner Core Conditions

Although studies on fcc FeH in the Earth's core are gaining momentum (Hikosaka et al., 2022; Ikuta et al., 2019; Kato et al., 2020; Tagawa et al., 2022a, 2022b; Thompson et al., 2018; Yang et al., 2022a, 2023), there are few reports on its elastic properties, especially its elastic properties under the extreme temperature and pressure conditions of the Earth's inner core. In addition, the elastic properties of the hcp Fe-H system at core conditions have been reported by previous studies (Caracas, 2015a; He et al., 2022a; Wang et al., 2021) but these studies reached different conclusions about the elastic properties of H on hcp Fe and so further examination is necessary. Here, we performed AIMD simulations to calculate the elastic properties of FeH as a function of temperature at 360 GPa. The calculated elastic constants C_{ij}, density ρ, adiabatic bulk modulus K_s, shear modulus G, compressional wave velocities V_p, shear wave velocities V_s, Debye sound velocities V_d, and Poisson's ratio ν are shown in Table S7 in Supporting Information S1 and Figure 4.

As shown in Table S7 in Supporting Information S1, all the elastic constants of Fe-H alloys show an almost linear variation with temperature. For fcc-FeH, C_{11}, C_{12}, and C_{44} decrease with increasing temperature; with the incorporation of H, C_{11} and C_{12} decrease but C_{44} increases when H vibrates around lattice sites and decreases when it becomes superionic in comparison with the pure hcp Fe. For hcp-FeH, C_{11}, C_{12}, C_{33}, and C_{44} exhibit similar behavior to pure hcp Fe by decreasing with temperature, while C_{13} displays the opposite behavior by increasing with temperature. Besides, C_{11}, C_{12}, C_{33}, and C_{44} of hcp Fe decrease with the presence of H but increase in C_{13}.

When considering the effect of H on seismic properties we compared it to a pure Fe hcp structure. We find that if FeH is in the hcp structure then the shear modulus G and shear wave velocities V_s decrease by ~51% and ~26%,
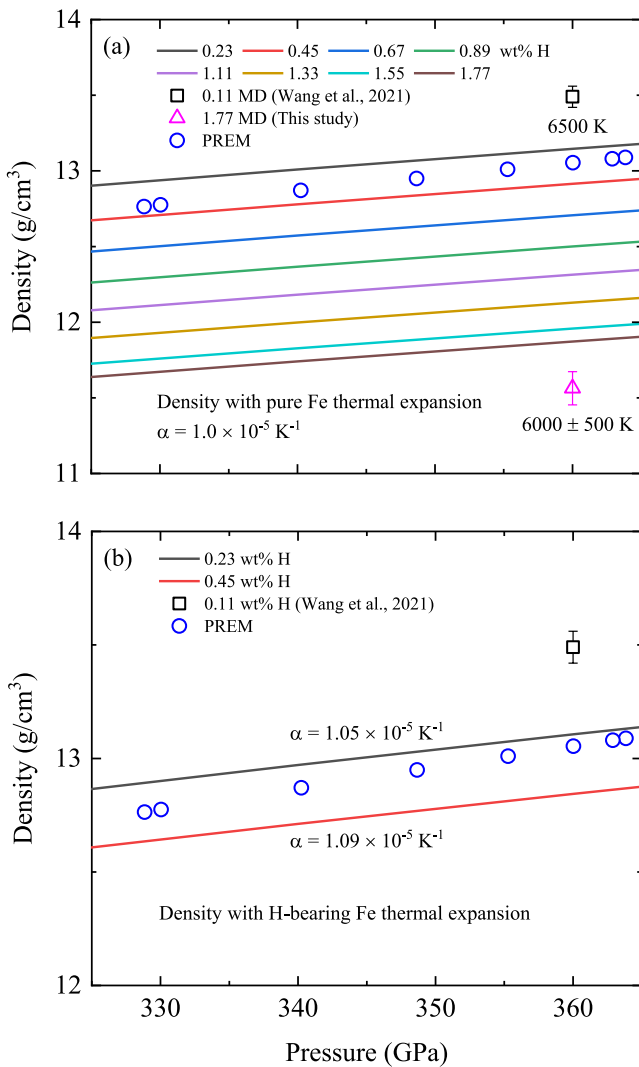
Figure 3. The H content required to reproduce the density of the Earth's inner core based on face-centered cubic (fcc) H-bearing Fe alloys. (a) Constrained inner core H content based on the thermal expansion of pure Fe. (b) Re-constrained inner core H content based on the thermal expansion of H-bearing Fe calculated from our MD calculations. The theoretical density of solid hexagonal close-packed (hcp) $Fe_{64}H_4$ with 0.11 wt % H (Wang et al., 2021) is also plotted for comparison.

respectively at a temperature of 5000 K. If FeH is in the fcc structure, these decreases in G and V_s are ~35% and ~19%, respectively (Figure 4 and Table S7 in Supporting Information S1). Such behavior is useful for explaining the core which has softer seismic velocities than pure Fe. This softening only exists at high temperatures. Under static conditions, we predict that H hardens Fe, with a V_p and a V_s that are ~5% and ~7% higher respectively in fcc FeH than in pure Fe. This difference is likely due to the superionic nature of H at high temperatures and explains the discrepancy in the literature where low-temperature studies predict H to harden the core (Caracas, 2015a).

Compared with our MD calculated results, the experimental data extrapolated from ambient temperature by Wakamatsu et al. (2022) overvalued the density and underestimated the compressional wave velocity V_p of fcc FeH at inner core conditions (Figure 4). The Debye sound velocities V_d of fcc FeH are always higher than those of hcp FeH even at high temperatures of 5000 K (Figure S5 and Table S7 in Supporting Information S1). This is in contrast to the predictions of Isaev et al. (2007) where fcc FeH had lower V_d than hcp FeH. These were based on low pressures and temperatures, however, and thus likely do not consider the superionic nature of H.

Thus we clarify the different conclusions about the elastic properties of H on solid Fe, where we show that a lattice H (by which we mean H vibrates around a singular point of the crystal lattice) hardens wave velocities of Fe while superionic H softens it (Caracas, 2015a; He et al., 2022a; Wang et al., 2021). 1 wt% of H would decrease the density of pure Fe by ~1.13 g/cm³, the V_p by ~0.31 km/s, and the V_s by ~1.01 km/s at the high P-T conditions of the inner core (360 GPa, 5000–6000 K). The Poisson's ratio of pure Fe increases with the incorporation of H at high temperatures, which is consistent with the early studies (He et al., 2022a; Wang et al., 2021). Both fcc- and hcp-FeH could explain the wave velocities (V_p and V_s) of the inner core although the concurrent density is still lower than the geophysical observations (Figure 4). Additionally, FeH can match the Debye sound velocities as well as the Poisson's ratio of the Earth's inner core (Figures S5 and S6 in Supporting Information S1). The FeH phase, as an end-member of the FeH_x ($x \leq 1$) system, is expected to be stable at the P-T conditions of the Earth's core. This work holds a key promise for superionic H to explain the seismic characteristics of the Earth's core, supporting the hypothesis that H is a vital light element in the core.

3.4. Implications for FeH and H in Earth's Inner Core

Both recent experiments and theoretical calculations have given strong evidence that the Earth's core is a potentially huge water reservoir with several oceans of water being brought into the Earth's interior during its formation (Hikosaka et al., 2022; Iizuka-Oku et al., 2017; Li et al., 2020; Nomura et al., 2014; Tagawa et al., 2021). These studies all support that H is a vital light element in the Earth's core, and therefore, the phase diagram of Fe-H at high P-T conditions is important for understanding the behavior as well as the process of H and/or water evolution in the early Earth. The phase diagram of the Fe-H system at high P-T conditions is similar to that of pure Fe (Sakamaki et al., 2009; Shen et al., 1998), the difference between them is that the hcp phase in pure Fe systems is substituted by the dhcp- or fcc-FeH in Fe-H systems (Kato et al., 2020; Pépin et al., 2014). It should be noted that the temperature and pressure of the two triple points (bcc-fcc-dhcp and fcc-dhcp-melt) of the Fe-H system are lower than those of the pure Fe system (Sakamaki et al., 2009). The phase boundary between dhcp and fcc in the Fe-H system is still controversial. Kato et al. (2020) observed that fcc FeH_x (x ~1) formed from dhcp at a pressure range of 57–137 GPa and 1000 K and that there was a negatively correlated slope of dT/dP at the phase boundary of dhcp-fcc. Their experiments also showed that hcp FeH_x with x ~1 was not stable at these relatively low P-T conditions. Our results
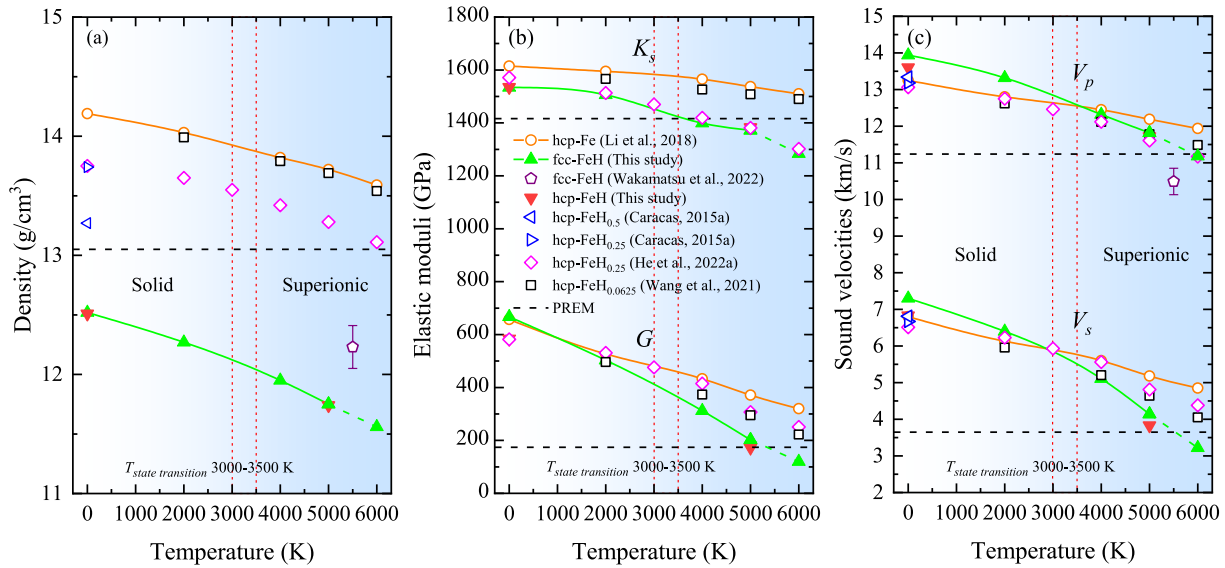
Figure 4. Density (a), elastic properties (b), and sound velocities (c) of H-bearing Fe alloys as a function of temperature at 360 GPa comparison with the PREM model (Dziewonski & Anderson, 1981). The theoretical data of pure hexagonal close-packed (hcp) Fe are from Li et al. (2018); hcp $FeH_{0.5}$ from Caracas (2015a); hcp $FeH_{0.25}$ from Caracas (2015a) and He et al. (2022a); and hcp $FeH_{0.625}$ from Wang et al. (2021). The extrapolated experimental data for face-centered cubic (fcc) FeH are from Wakamatsu et al. (2022). The data of fcc FeH under 6000 K are fitted from data at 0, 2000, 4000, and 5000 K. The red dashed line region represents the superionic state transition temperature for hcp Fe-H (~3000 K) (He et al., 2022a) and fcc Fe-H (~3500 K) (Yang et al., 2022a).

demonstrate the formation of H-poor hcp and H-rich fcc phases FeH_x at core pressure conditions, while high temperatures are likely to favor the hcp phase in the Earth's inner core (Figure 1b). These results are important to understand the H behavior under core conditions and also put an anchor in the experimental and theoretical study of the Fe-H phase diagram.

Although we predict that the hcp-FeH is favored at high temperatures of the Earth's inner core, the discussion and further study of fcc-FeH is still necessary. We predict a small difference between the energy of the two phases (on the order of 10 s meV/atom) which is smaller than $k_B T$ at these temperatures. This implies that small changes to composition (e.g., varying H concentration or possibly the effect of other elements such as Ni and Si) or temperature could induce phase changes in the core meaning both phases are thermodynamically or kinetically possible. Both the fcc and hcp phase FeH can explain the geophysical requirements for light elements in the inner core to soften the shear modulus, decrease the sound wave velocities, and increase the Poisson's ratio of Fe at inner core conditions. The superionic H in Fe hcp lattice has a stronger softening in G and V_s compared with that in Fe fcc lattice, which suggests that to match the V_s of the inner core an hcp FeH_x may require a lower temperature or a less H concentration. Based on the density, the H content in the inner core can be constrained to ~0.26–0.34 wt% assuming H as the only light element.

4. Conclusions

Calculations of the energy differences between fcc and hcp FeH_x phases suggest that hcp is favored in H-poor and fcc in H-rich conditions and that increasing temperature favors the hcp phase. The free energy difference between these two phases at inner core conditions is predicted, however, to be very small (on the order of 10 s meV/atom) and thus there is a possibility of the coexistence of H-bearing hcp- and fcc-Fe in the inner core. At high temperatures of the Earth's inner core, H is predicted to be superionic and this has the effect of softening the elasticity of Fe, an effect which will not be observed in low-temperature measurements. Finally, we clarify that lattice H hardens the wave velocities of Fe while temperature-induced superionic H softens it. Both fcc- and hcp-FeH could explain inner-core wave velocities and Poisson's ratio. We conclude H could play an important role in the real core.

Data Availability Statement

Supporting Information S1 is included in seven figures and seven tables. The source code (VASP) used in this study is available at https://www.vasp.at/. According to AGU data policy, raw data are available at https://doi.org/10.6084/m9.figshare.24047208.v2. Additional data for Figure 1 was sourced from Vočadlo et al. (2008).

Data for Figure 2 was sourced from Caracas (2015b), Dewaele et al. (2006), Tagawa et al. (2022c), Tsujino et al. (2013), and Yang et al. (2022b). Data for Figure 3 was sourced from Dziewonski and Anderson (1981) and Wang et al. (2021). Data for Figure 4 was sourced from Caracas (2015b), Dziewonski and Anderson (1981), He et al. (2022b), Li et al. (2018), Wakamatsu et al. (2022), and Wang et al. (2021). Note that other citation data that do not provide Datasets are taken directly from the text or the supplementary material of the references.

References

Anderson, O. L. (2003). The three-dimensional phase diagram of iron. In V. Dehant, K. C. Creager, S.-I. Karato, & S. Zatman (Ed.), *Earth's core: Dynamics, structure, rotation*. American Geophysical Union.

Belonoshko, A. B., Lukinov, T., Fu, J., Zhao, J., Davis, S., & Simak, S. I. (2017). Stabilization of body-centred cubic iron under inner-core conditions. *Nature Geoscience*, *10*(4), 312–316. https://doi.org/10.1038/NGEO2892

Belonoshko, A. B., Simak, S. I., Olovsson, W., & Vekilova, O. Y. (2022). Elastic properties of body-centered cubic iron in Earth's inner core. *Physical Review B*, *105*(18), L180102. https://doi.org/10.1103/PhysRevB.105.L180102

Blöchl, P. E. (1994). Projector augmented-wave method. *Physical Review B*, *50*(24), 17953–17979. https://doi.org/10.1103/PhysRevB.50.17953

Caracas, R. (2015a). The influence of hydrogen on the seismic properties of solid iron. *Geophysical Research Letters*, *42*(10), 3780–3785. https://doi.org/10.1002/2015GL063478

Caracas, R. (2015b). The influence of hydrogen on the seismic properties of solid iron [Dataset]. Earthref. Retrieved from http://earthref.org/ERDA/download:1924

Côté, A., Vočadlo, L., & Brodholt, J. P. (2008). The effect of silicon impurities on the phase diagram of iron and possible implications for the Earth's core structure. *Journal of Physics and Chemistry of Solids*, *69*(9), 2177–2181. https://doi.org/10.1016/j.jpcs.2008.03.031

Desjarlais, M. P. (2013). First-principles calculation of entropy for liquid metals. *Physical Review E*, *88*(6), 062145. https://doi.org/10.1103/PhysRevE.88.062145

Dewaele, A., Loubeyre, P., Occelli, F., Mezouar, M., Dorogokupets, P. I., & Torrent, M. (2006). Quasihydrostatic equation of state of Iron above 2 Mbar. *Physical Review Letters*, *97*(21), 29–32. https://doi.org/10.1103/PhysRevLett.97.215504

Dziewonski, A. M., & Anderson, D. L. (1981). Preliminary reference Earth model. *Physics of the Earth and Planetary Interiors*, *25*(4), 297–356. https://doi.org/10.17611/DP/9991844

Flyvbjerg, H., & Petersen, H. G. (1989). Error estimates on averages of correlated data. *Journal of Chemical Physics*, *91*(1), 461–466. https://doi.org/10.1063/1.457480

Fukai, Y. (1984). The iron–water reaction and the evolution of the Earth. *Nature*, *308*(5955), 174–175. https://doi.org/10.1038/308174a0

Gomi, H., Fei, Y., & Yoshino, Y. (2018). The effects of ferromagnetism and interstitial hydrogen on the equation of states of hcp and dhcp FeH_x: Implications for the Earth's inner core age. *American Mineralogist*, *103*(8), 1271–1281. https://doi.org/10.2138/am-2018-6295

He, Y., Sun, S., Kim, D. Y., Bo, G. J., & Mao, H. K. (2022a). Superionic hcp-Fe alloys and their seismic velocities in Earth's inner core. *Nature*, *602*, 258–262. https://doi.org/10.1038/s41586-021-04361-x

He, Y., Sun, S., Kim, D. Y., Bo, G. J., & Mao, H. K. (2022b). Superionic hcp-Fe alloys and their seismic velocities in Earth's inner core [Dataset]. 4TU.ResearchData. https://doi.org/10.4121/12932588.v2

Hikosaka, K., Tagawa, S., Hirose, K., Okuda, Y., Oka, K., Umemoto, K., & Ohishi, Y. (2022). Melting phase relations in Fe–Si–H at high pressure and implications for Earth's inner core crystallization. *Scientific Reports*, *12*, 10000. https://doi.org/10.1038/s41598-022-14106-z

Hirose, K., Tagawa, S., Kuwayama, Y., Sinmyo, R., Morard, G., Ohishi, Y., & Genda, H. (2019). Hydrogen limits carbon in liquid iron. *Geophysical Research Letters*, *46*(10), 5190–5197. https://doi.org/10.1029/2019GL082591

Hirose, K., Wood, B., & Vočadlo, L. (2021). Light elements in the Earth's core. *Nature Reviews Earth & Environment*, *2*, 645–658. https://doi.org/10.1038/s43017-021-00203-6

Hohenberg, P., & Kohn, W. (1964). Inhomogeneous electron gas. *Physical Review*, *136*(3B), B864–B871. https://doi.org/10.1103/PhysRev.136.B864

Iizuka-Oku, R., Yagi, T., Gotou, H., Okuchi, T., Hattori, T., & Sano-Furukawa, A. (2017). Hydrogenation of iron in the early stage of Earth's evolution. *Nature Communications*, *8*, 14096. https://doi.org/10.1038/ncomms14096

Ikuta, D., Ohtani, E., Sano-Furukawa, A., Shibazaki, Y., Terasaki, H., Yuan, L., & Hattori, T. (2019). Interstitial hydrogen atoms in face-centered cubic iron in the Earth's core. *Scientific Reports*, *9*, 7108. https://doi.org/10.1038/S41598-019-43601-Z

Isaev, E. I., Skorodumova, N. V., Ahuja, R., Vekilov, Y. K., & Johansson, B. (2007). Dynamical stability of Fe-H in the Earth's mantle and core regions. *Proceedings of the National Academy of Sciences*, *104*(22), 9168–9171. https://doi.org/10.1073/pnas.0609701104

Karki, B. B., Stixrude, L., & Wentzcovitch, R. M. (2001). High-pressure elastic properties of major materials of Earth's mantle from first principles. *Reviews of Geophysics*, *39*(4), 507–534. https://doi.org/10.1029/2000RG000088

Kato, C., Umemoto, K., Ohta, K., Tagawa, S., & Ohishi, Y. (2020). Stability of fcc phase FeH to 137 GPa. *American Mineralogist*, *105*(6), 917–921. https://doi.org/10.2138/am-2020-7153

Kohn, W., & Sham, L. J. (1965). Self-consistent equations including exchange and correlation effects. *Physical Review*, *140*(4A), A1133–A1138. https://doi.org/10.1103/physrev.140.a1133

Kresse, G., & Furthmüller, J. (1996). Efficient iterative schemes for ab initio total-energy calculations using a plane-wave basis set. *Physical Review B*, *54*(16), 11169–11186. https://doi.org/10.1103/physrevb.54.11169

Lai, P. K., Hsieh, C. M., & Lin, S. T. (2012). Rapid determination of entropy and free energy of mixtures from molecular dynamics simulations with the two-phase thermodynamic model. *Physical Chemistry Chemical Physics*, *14*(43), 15206–15213. https://doi.org/10.1039/c2cp42011b

Li, Y., Guo, X., Vočadlo, L., Brodholt, J. P., & Ni, H. (2022). The effect of water on the outer core transport properties. *Physics of the Earth and Planetary Interiors*, *329–330*, 106907. https://doi.org/10.1016/j.pepi.2022.106907

Li, Y., Vočadlo, L., & Brodholt, J. P. (2018). The elastic properties of hcp-Fe alloys under the conditions of the Earth's inner core. *Earth and Planetary Science Letters*, *493*, 118–127. https://doi.org/10.1016/j.epsl.2018.04.013

Li, Y., Vočadlo, L., & Brodholt, J. P. (2022). ElasT: A toolkit for thermoelastic calculations. *Computer Physics Communications*, *273*, 108280. https://doi.org/10.1016/j.cpc.2021.108280

Li, Y., Vočadlo, L., Sun, T., & Brodholt, J. P. (2020). The Earth's core as a reservoir of water. *Nature Geoscience*, *13*, 1–6. https://doi.org/10.1038/s41561-020-0578-1

Lin, S.-T., Blanco, M., & Goddard, W. A. (2003). The two-phase model for calculating thermodynamic properties of liquids from molecular dynamics: Validation for the phase diagram of Lennard-Jones fluids. *The Journal of Chemical Physics*, *119*(22), 11792–11805. https://doi.org/10.1063/1.1624057

Lodders, K. (2003). Solar system abundances and condensation temperatures of the elements. *The Astrophysical Journal*, *591*(2), 1220–1247. https://doi.org/10.1086/375492

Mermin, N. D. (1965). Thermal properties of the inhomogeneous electron gas. *Physical Review*, *137*(5A), 1441–1443. https://doi.org/10.1103/PhysRev.137.A1441

Monkhorst, H. J., & Pack, J. D. (1976). Special points for Brillouin-zone integrations. *Physical Review B*, *16*(4), 1748–1749. https://doi.org/10.1103/PhysRevB.13.5188

Narygina, O., Dubrovinsky, L. S., McCammon, C. A., Kurnosov, A., Kantor, I. Y., Prakapenka, V. B., & Dubrovinskaia, N. A. (2011). X-ray diffraction and Mössbauer spectroscopy study of fcc iron hydride FeH at high pressures and implications for the composition of the Earth's core. *Earth and Planetary Science Letters*, *307*(3–4), 409–414. https://doi.org/10.1016/j.epsl.2011.05.015

Nomura, R., Hirose, K., Uesugi, K., Ohishi, Y., Tsuchiyama, A., Miyake, A., & Ueno, Y. (2014). Low core-mantle boundary temperature inferred from the solidus of pyrolite. *Science*, *343*(6170), 522–525. https://doi.org/10.1126/science.1248186

Nosé, S. (1984). A molecular dynamics method for simulations in the canonical ensemble. *Molecular Physics*, *52*(2), 255–268. https://doi.org/10.1080/00268978400101201

Ohtani, E., Hirao, N., Kondo, T., Ito, M., & Kikegawa, T. (2005). Iron-water reaction at high pressure and temperature, and hydrogen transport into the core. *Physics and Chemistry of Minerals*, *32*(1), 77–82. https://doi.org/10.1007/s00269-004-0443-6

Oka, K., Tagawa, S., Hirose, K., & Ohishi, Y. (2022). Melting experiments on Fe-O-H: Evidence for eutectic melting in Fe-FeH and Implications for hydrogen in the core. *Geophysical Research Letters*, *49*(17), e2022GL099420. https://doi.org/10.1029/2022GL099420

Okuchi, T. (1997). Hydrogen partitioning into molten iron at high pressure: Implications for Earth's core. *Science*, *278*(5344), 1781–1784. https://doi.org/10.1126/science.278.5344.1781

Pépin, C. M., Dewaele, A., Geneste, G., Loubeyre, P., & Mezouar, M. (2014). New Iron hydrides under high pressure. *Physical Review Letters*, *113*(26), 265504. https://doi.org/10.1103/PhysRevLett.113.265504

Perdew, J. P., Burke, K., & Ernzerhof, M. (1996). Generalized gradient approximation made simple. *Physical Review Letters*, *77*(18), 3865–3868. https://doi.org/10.1103/PhysRevLett.77.3865

Poirier, J. P. (1994). Light elements in the Earth's outer core: A critical review. *Physics of the Earth and Planetary Interiors*, *85*(3–4), 319–337. https://doi.org/10.1016/0031-9201(94)90120-1

Sakamaki, K., Takahashi, E., Nakajima, Y., Nishihara, Y., Funakoshi, K., Suzuki, T., & Fukai, Y. (2009). Melting phase relation of FeH$_x$ up to 20 GPa: Implication for the temperature of the Earth's core. *Physics of the Earth and Planetary Interiors*, *174*(1–4), 192–201. https://doi.org/10.1016/j.pepi.2008.05.017

Schneider, T., & Stoll, E. (1978). Molecular-dynamics study of a three-dimensional one-component model for distortive phase transitions. *Physical Review B*, *17*(3), 1302–1322. https://doi.org/10.1103/PhysRevB.17.1302

Shen, G., Mao, H. K., Hemley, R. J., Duffy, T. S., & Rivers, M. L. (1998). Melting and crystal structure of iron at high pressures. *Geophysical Research Letters*, *25*(3), 373–376. https://doi.org/10.1029/97GL03776

Shibazaki, Y., Ohtani, E., Terasaki, H., Suzuki, A., & Funakoshi, K. I. (2009). Hydrogen partitioning between iron and ringwoodite: Implications for water transport into the Martian core. *Earth and Planetary Science Letters*, *287*(3), 463–470. https://doi.org/10.1016/j.epsl.2009.08.034

Simmons, G., & Wang, H. (1971). *Single crystal elastic constants and calculated aggregate properties: A handbook*. MIT Press.

Tagawa, S., Gomi, H., Hirose, K., & Ohishi, Y. (2022a). High-temperature equation of state of FeH: Implications for hydrogen in Earth's Inner core. *Geophysical Research Letters*, *49*(5), e2021GL096260. https://doi.org/10.1029/2021GL096260

Tagawa, S., Helffrich, G., Hirose, K., & Ohishi, Y. (2022b). High-pressure melting curve of FeH: Implications for eutectic melting between Fe and non-magnetic FeH. *Journal of Geophysical Research: Solid Earth*, *127*(6), e2022JB024365. https://doi.org/10.1029/2022jb024365

Tagawa, S., Gomi, H., Hirose, K., & Ohishi, Y. (2022c). High-temperature equation of state of FeH: Implications for hydrogen in Earth's Inner core [Dataset]. Zenondo. https://doi.org/10.5281/zenodo.5513718

Tagawa, S., Sakamoto, N., Hirose, K., Yokoo, S., Hernlund, J., Ohishi, Y., & Yurimoto, H. (2021). Experimental evidence for hydrogen incorporation into Earth's core. *Nature Communications*, *12*, 2588. https://doi.org/10.1038/s41467-021-22035-0

Thompson, E. C., Davis, A. H., Bi, W., Zhao, J., Alp, E. E., Zhang, D., et al. (2018). High-pressure geophysical properties of fcc phase FeH$_x$. *Geochemistry, Geophysics, Geosystems*, *19*(1), 305–314. https://doi.org/10.1002/2017GC007168

Tsujino, N., Nishihara, Y., Nakajima, Y., Takahashi, E., Funakoshi, K., & Higo, Y. (2013). Equation of state of γ-Fe: Reference density for planetary cores. *Earth and Planetary Science Letters*, *375*, 244–253. https://doi.org/10.1016/j.epsl.2013.05.040

Vočadlo, L. (2007). Ab initio calculations of the elasticity of iron and iron alloys at inner core conditions: Evidence for a partially molten inner core? *Earth and Planetary Science Letters*, *254*(1–2), 227–232. https://doi.org/10.1016/j.epsl.2006.09.046

Vočadlo, L., Alfè, D., Gillan, M. J., & Price, G. D. (2003). The properties of iron under core conditions from first principles calculations. *Physics of the Earth and Planetary Interiors*, *140*(1–3), 101–125. https://doi.org/10.1016/j.pepi.2003.08.001

Vočadlo, L., Wood, I. G., Alfè, D., & Price, G. D. (2008). Ab initio calculations on the free energy and high *P–T* elasticity of face-centred-cubic iron. *Earth and Planetary Science Letters*, *268*(3–4), 444–449. https://doi.org/10.1016/j.epsl.2008.01.043

Wakamatsu, T., Ohta, K., Tagawa, S., Yagi, T., Hirose, K., & Ohishi, Y. (2022). Compressional wave velocity for iron hydrides to 100 gigapascals via picosecond acoustics. *Physics and Chemistry of Minerals*, *49*(5), 17. https://doi.org/10.1007/s00269-022-01192-8

Wang, W., Li, Y., Brodholt, J. P., Voadlo, L., & Wu, Z. (2021). Strong shear softening induced by superionic hydrogen in Earth's inner core. *Earth and Planetary Science Letters*, *568*(6131), 117014. https://doi.org/10.1016/j.epsl.2021.117014

Wilson, A., & Stixrude, L. (2021). Entropy, dynamics, and freezing of CaSiO$_3$ liquid. *Geochimica et Cosmochimica Acta*, *302*, 1–17. https://doi.org/10.1016/j.gca.2021.03.015

Yang, H., Muir, J. M. R., & Zhang, F. (2022a). Iron hydride in the Earth's inner core and its geophysical implications. *Geochemistry, Geophysics, Geosystems*, *23*(12), e2022GC010620. https://doi.org/10.1029/2022gc010620

Yang, H., Muir, J. M. R., & Zhang, F. (2022b). Iron hydride in the Earth's Inner core and its geophysical implications [Dataset]. Figureshare. https://doi.org/10.6084/m9.figshare.20765965.v1

Yang, H., Muir, J. M. R., & Zhang, F. (2023). Volumes and spin states of FeH$_x$: Implication for the density and temperature of the Earth's core. *American Mineralogist*, *180*(4), 667–674. https://doi.org/10.2138/am-2022-8237

Ye, Q.-J., Zhuang, L., & Li, X.-Z. (2021). Dynamic nature of high-pressure ice VII. *Physical Review Letters*, *126*(18), 185501. https://doi.org/10.1103/PhysRevLett.126.185501

Yuan, L., Ohtani, E., Ikuta, D., Kamada, S., Tsuchiya, J., Naohisa, H., et al. (2018). Chemical reactions between Fe and H$_2$O up to megabar pressures and Implications for water storage in the Earth's mantle and core. *Geophysical Research Letters*, *45*(3), 1330–1338. https://doi.org/10.1002/2017gl075720